Global properties of X-ray afterglows of GRB(*)

L. Piro

INAF, Istituto Astrofisica Spaziale e Fisica Cosmica - Rome, Italy

Summary. — In this paper we review the general properties of X-ray afterglows. We discuss in particular on the powerful diagnostics provided by X-ray afterglows in constraining the environment and fireball in normal GRB, and the implications on the origin of dark GRB and XRF. We also discuss on the observed properties of the transition from the prompt to the afterglow phase, and present a case study for a late X-ray outburst interpreted as the onset of the afterglow stage.

PACS 95.85.Nv – X-ray.
PACS 98.70.Rz – γ-ray sources; γ-ray bursts.
PACS 01.30.Cc – Conference proceedings.

1. – X-ray features

The presence of X-ray features is an issue with important implications on the origin of the progenitor and on the cosmological use of GRB (see [20] for a review). So far, different authors reported evidence, ranging from 2.8 to 4.7 sigma significance, in six objects for features associated to iron complex (see [20] and reference therein), and in 3–4 objects for lines associated to lower-Z elements (Mg, Si, S, Ar) [26,31,1,30]. For what regards iron features, when an independent redshift measurement is available, the emission features in the afterglow phase are consistent with highly ionized iron, while in the prompt phase the absorption feature corresponds to neutral stage, suggesting a temporal evolution guided by the large increase of ionization produced by GRB photon field [19]. The strong dependence of the line efficiency on the ionization stage of the material, variable over orders of magnitude from the prompt to the afterglow phase, can explain the transitory presence of lines in a same object or the tighter upper limits derived in some other bursts. In this framework soft–X-ray lines and iron lines are mutually exclusive, because their maximum efficiencies are achieved at a different ionization parameter [16]. While the present body of observations can thus be consistent with theoretical expectations, the

---

(*) Paper presented at the "4th Workshop on Gamma-Ray Burst in the Afterglow Era", Rome, October 18-22, 2004.
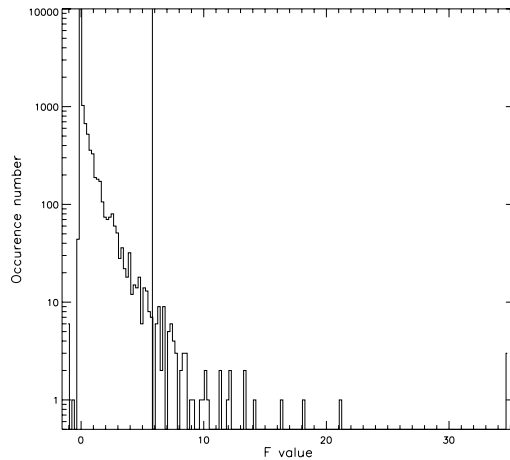
Fig. 1. – Monte Carlo simulations of F-variable distribution for the BeppoSAX observation of GRB970508 for the null model (power law without line). The vertical line identifies the observed value of the F-variable after the addition of a line, that corresponds to a probability of a chance fluctuation of 0.4%.

former is still sparse, and more data, of higher statistical quality, are required. Here we briefly discuss about the methods to assess the statistical significance of these features. Usually this is derived by using the F-test. According to [25] the F-variable does not follow the F distribution when the boundary of the normalization of an additional model component is zero, as it is the case of emission or absorption features. In such a case the correct probability distribution of the F-variable is to be derived by using Monte Carlo (MC) simulations of the null (*i.e.* the continuum) model. For each MC realization of the null model, the value of the F-variable is then derived by fitting the simulated spectrum with the continuum model and then with the addition of the line (hereafter we refer to this method with SP, standard prescription). The authors in [27] carried out a systematic analysis of several afterglows, including all those with reported evidence of features. However they did not apply the aforementioned SP but devised a different method, obtaining a much lower statistical significance than reported in "discovery" papers. They claim that, while the SP is in principle correct, in practice it fails in a blind search of several lines, due to the inadequacy of χ^2 minimization routines to find the absolute minimum. We have applied the SP to a single line at a given energy, *i.e.* a case not affected by minimization convergence, specifically to the case of GRB970508. The results of the different methods are thus compared *under the same assumption, i.e.* single trial probability. Our result with the SP is presented in fig. 1. It gives a statistical significance of 99.6%. This is actually slightly better than the 99.3%, originally derived in [22] by applying the F-test. On the contrary [27] derive a significance of 60%. The same data were also reanalyzed in [25], which derive a 99.3% significance by applying the SP, consistent with our estimation.

As originally noted in [25], the F-test slightly *underestimates* the significance of an emission feature. We also note that in XSPEC the χ^2 computation with the default setting adopts errors derived from observed counts, while the correct formula (that can be selected in the program, but requires the background file) requires the variance to be computed from the model [32]. This leads to an underestimation of the significance
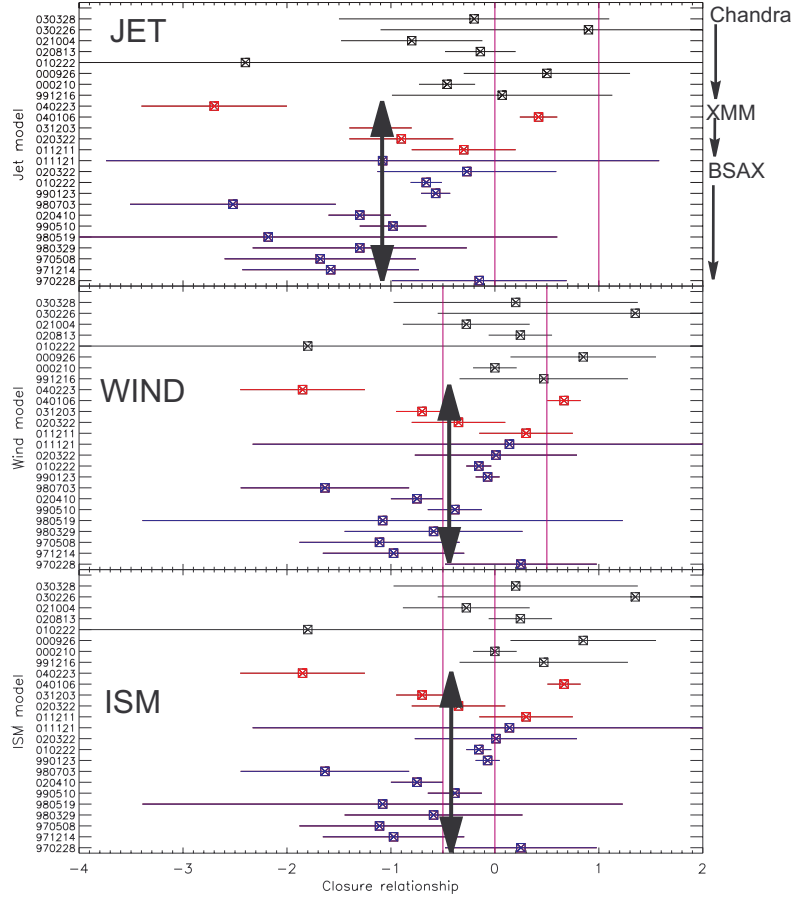
Fig. 2. – Distribution of the values of the closure relationships for jet (upper panel), spherical expansion in ISM (mid panel) and wind (lower panel). The sample includes afterglows observed with Chandra, XMM and BeppoSAX. The vertical lines are the expected values for $\nu > \nu_c$ (left) and $\nu < \nu_c$ (right). The arrows identify the average value derived for the combined BeppoSAX and XMM sample. They are consistent with ISM or wind expansion with $\nu > \nu_c$.

of deviations above the continuum, *i.e.* of emission lines, and to an overestimation of deviations below the continuum (absorption feature) the more severe when the equivalent width is large and the spectrum is source-dominated. We therefore conclude that the statistical significance derived by using the F-test, at least in the case of single line searched in a narrow range, gives a conservative estimation of the confidence level of an emission feature. An extension of the work to blind searches for multiple lines (soft–X-ray lines) is in progress.

2. – Afterglow evolution and constraints on the fireball and environment

In previous papers [20, 5] we have shown that the application of closure relationship derived from spectral and temporal evolution of X-ray afterglows by BeppoSAX set relevant contraints on the fireball model and the environment. In particular we derived
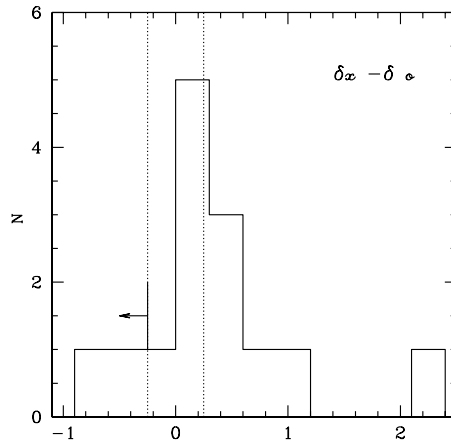
Fig. 3. – Distribution of the difference of decay indeces of X-ray and optical afterglows ($\delta_X - \delta_O$) for the BeppoSAX sample. The two dashed lines identify the expected value for a ISM ($\delta_X - \delta_O = 0.25$) and a wind ($\delta_X - \delta_O = -0.25$).

that the fireball at $t \leq 1$–2 days does not (yet) show evidence of collimated flow, and is consistent with a spherical expansion with a cooling frequency below the X-ray range. We are extending this analysis including the XMM and Chandra observations. The results are summarized in fig. 2. We note that the XMM data are fully consistent with the BSAX sample. Indeed, the typical observing time by XMM is similar to that of BeppoSAX (few hours–2 days). In the case of Chandra, there is a significant difference in the closure relationship, with the Chandra sample consistent with a jet flow [11]. This apparent inconsistency is likely due to the fact that Chandra observations start on average at later times, and that the effects of jet flow on the light curve (*i.e.* the break time) take place around 2–3 days.

Density profiles derived from broad-band afterglow modelling are particularly intriguing, in that the majority of events are consistent with a constant density environment, and only in few cases a wind profile is clearly preferred [2, 18]. This is at odd with the simple expectation of massive star progenitors. Recently [3] proposed a solution to solve this discrepancy, arguing that a region of constant density would be produced at the boundary of the wind with the molecular cloud surrounding the progenitor.

What can we tell about this issue from X-ray afterglows? When the cooling frequency is above the X-ray band, as it happens in the majority of the cases, the closure relationship for wind and ISM are degenerate (fig. 2). One notable exception is GRB040106 [12] where ν_c is below the X-ray band and the combined spectral and temporal evolution in X-rays indicates a wind profile. The addition of the optical temporal evolution provides a powerful indicator to tell the ISM *vs.* wind environment. In a wind profile the decay in X-rays should be shallower than in the optical, while the reverse holds true in a constant density environment (ISM). The absolute value of the difference of the decay slopes is 0.25. In fig. 3 we plot the difference in decay slopes $\delta_X - \delta_O$ for the BeppoSAX sample. This shows that the ISM profile is preferred in most of the cases. One intriguing outlier (see next section) is GRB011121 [21]. In this event we derived $\delta_X = 1.29 \pm 0.04$ *vs.* $\delta_O = 1.66 \pm 0.06$ observed by [24], consistent only with a wind profile, as also suggested in [24] by comparing optical and radio data. Another wind-profile candidate is presented in [10].

3. – Early and delayed afterglows and the transition from the prompt phase

Early papers combining the BeppoSAX WFC and NFI [8] have outlined a clear separation in between two phases of the GRB emission. The prompt phase is characterized by a hard spectrum with a strong hard-to-soft spectral evolution. This is followed, on a time scale of tens of seconds, by a second phase with a soft spectrum, well described by a power law with spectral index $\alpha \sim 1$ with no substantial spectral variation. This phase is associated with the onset of the afterglow on the bases of two pieces of evidence. First, the X-ray spectrum is similar to that observed in the late afterglow at 1 day. Second, the X-ray flux falls on the backward extrapolation of the late afterglow light curve. The prompt and early afterglow phases can be separated by temporal gaps or can be mixed [29] but, so far, the transition has been always observed within tens of seconds from the onset of the prompt emission.

In few cases, however, the transition appears to take place on a much longer time scale. In a recent paper [21] have present evidence of an X-ray burst starting hundreds of seconds after the prompt phase in two bursts, GRB011121 and GRB011211 (see also [10] for XRF011030) has been presented. In the November burst the spectrum of the late X-ray burst was markedly softer than that of the preceding emission and was similar to that observed in the late afterglow observations. It is therefore tempting to identify the late X-ray bursting as the onset of the afterglow. Contrary to what observed for transitions on shorter time scales, the decay part of the late X-ray burst cannot be connected to the 1-day afterglow emission with a single power law $(t - t_0)^{-\delta_X}$ (fig. 4). *However, this is the case (fig. 4, right panel) when t_0 is set equal to the onset of the late X-ray burst.* This empirical result can be explained in the framework of the fireball model, taking into account the thickness of the shell. The onset of external shocks depends on the dynamical conditions of the fireball and, in particular, two regimes can be identified depending on the "thickness" of the fireball [28]. In the regime of thin shell, the reverse shock crosses the shell before the onset of the self-similar solution (*i.e.* when an ISM mass $m = M_0/\Gamma_0$ is collected, M_0 and Γ_0 being the rest mass and asymptotic Lorentz factor of the fireball, respectively). As a consequence, the onset of the afterglow coincides with the deceleration time. Moreover, the evolution of the afterglow after the peak is well described by a power law decay, if the time is measured starting from the explosion time, very well approximated by the time at which the first prompt phase photons are collected. In the case of a thick shell, the reverse shock has not crossed the shell when the critical mass $m = M_0/\Gamma_0$ has been collected, and therefore the external shock keeps being energized for a longer time. The peak of the afterglow emission therefore coincides with the shell crossing time of the reverse shock, equal to the duration of prompt phase. The afterglow decay will be well described with a single power law only if the time is measured starting from the time at which the inner engine turns off, roughly coincident with the GRB duration.

4. – Dark bursts

One of the most discussed issues of the field is the origin of the dark GRB [5]. A first estimation of the fraction of these events, around 50% of the whole population of GRB, was based adopting an upper limit on the optical magnitude at 1 day of around 22–23. The availability of fast and precise position, as *e.g.*, delivered by HETE2, has led to the detection of a few rapidly fainting optical transients, that would likely be classified as dark GRB with observations performed at later times [7]. Fynbo *et al.* [9] showed that
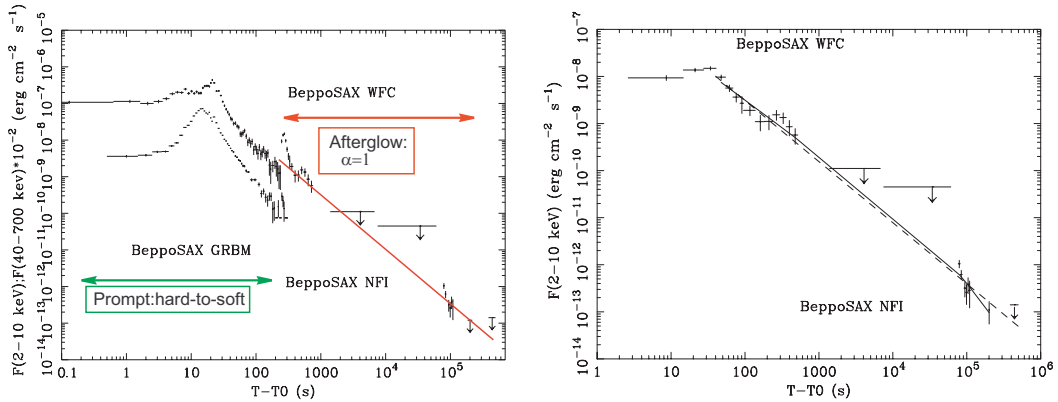
Fig. 4. – Light curves of GRB011121. On the left we show the curves of WFC, NFI and GRBM when t_0 is, as usual, set with the start of the prompt emission. Note that the outburst observed around 250 s lies above the power law describing the late afterglow emission. However, when t_0 is shifted to the onset of the outburst (right panel), the decay part of the outburst and the late afterglow fall on a same power law.

about 75% of dark GRB were consistent with no detection if they were similar to dim burst detected in the optical with deep searches. Thus, the original definition of a dark burst is affected by significant observational bias.

A more effective classification makes use of broad-band information. Let us consider a first set of causes that can make a burst optically dim. A fast decay, as it would be the case of a highly collimated jet is one possibility. They can also be intrinsically under-luminous events, or GRB located at distances higher than that of OTGRB, but at a redshift not greater than 5 (see below). *In all these cases the afterglow flux should scale by the same factor at all wavelengths.* Indeed [5] found that dark GRB are on average 6 times fainter in X-rays that OTGRB. Incidentally we note that this effect can account, at least in part, for the higher number of OTGRB identified by HETE2.

On the contrary, the optical flux of a GRB at $z \gtrsim 5$ or of a GRB in a dusty star-forming region should be depleted not only in absolute magnitude but also with respect to other wavelengths. Guided by this consideration, the authors in [5] have carried out a study of dark GRB *vs.* OTGRB comparing their X-ray *vs.* optical fluxes. In 75% of dark GRBs, the upper limits on the optical–to–X-ray flux ratio (f_{OX}) are consistent with the ratio observed in OTGRB, which is narrowly distributed around a optical–to–X-ray spectral index $\beta_{OX} = 0.8$ (that is, modulo a constant factor, the same as $\log(f_{OX})$). This population of events is therefore consistent with being OTGRB going undetected in the optical because searches were not fast or deep enough. However, for about 25% of dark GRB, f_{OX} is at least a factor 5–10 lower than the average value observed in OTGRB, and also lower than the smallest observed f_{OX}. In terms of spectral index, these events have $\beta_{OX} < 0.6$. Furthermore, the optical upper limits are also lower than the faintest optical afterglow. These GRB cannot be therefore explained as dim OTGRBs, and are named *truly dark or optically depleted GRB*.

We stress that the upper limit on f_{OX} for optically depleted GRB is model independent, being derived by a comparison with the optically bright GRB, where the f_{OX} distribution is rather narrow, clustering around the average value within a factor of 2 (the 1 sigma width). A similar value on the upper limit on f_{OX} has been derived in

two dark GRB [6,23] by modelling the broad-band data via the standard fireball model. Both of these events have been associated with host galaxies at $z \lesssim 5$, leading to the conclusion that the optical is depleted by dust in star-forming region.

A similar approach has been followed by [14]. They derived β_{OX} for a large sample of GRB and compared it with the expectations of the fireball model. They find that at least 10% of the objects of their sample have an optical flux (or upper limits) fainter than the minimum allowed by the model, corresponding to $\beta_{OX} < 0.5$–0.55, and similar to the *observed* limit derived by [5]. In conclusion, ≈ 10–20% of the burst population is characterized by an optical afterglow emission substantially fainter than that expected from the X-ray afterglow flux. As mentioned above this behaviour cannot be accounted by *achromatic* effects, such as jet expansion or luminosity. It requires causes that are selectively depleting the optical range with respect to X-rays, such as dust extinction in star-forming regions or absorption by Ly_α forest of GRB at $z > 5$. As noted above, in few events the likely explanation is dust extinction. The detection of high-z GRB is more challenging, since the light of the host galaxy should be extremely dim. The large number of SWIFT localizations should hopefully lead to the first identifications of high-z GRB.

5. – X-ray flashes

This new class of GRB was originally discovered by BeppoSAX [13], confirmed and extended by HETE2 [15]. Their origin is still to be understood and, on this issue, we would like to show some implications derived from the properties of X-ray afterglows of XRF when compared to those of normal GRB. The authors of [4] find that the distribution of X-ray fluxes (at 12 hours after the burst) of the two classes are consistent with each other. In particular the ratio of the average flux of the two populations is 1.2 ± 0.6. This result appears at odd with simple expectations by two popular scenarios. Let us first assume that XRF are normal GRB lying at larger distances. In such a case one would expect to observe a fainter afterglow, assuming that no selection effect biases the sample. For example, assuming an average redshift of 5 for XRF *vs.* $z = 1$ for GRB, the X-ray afterglow flux should be on average 7 times fainter in XRF, contrary to what is observed. Indeed we already know that some XRF are much closer (see references in [4]). Nonetheless, about 50% of the XRF for which optical observations were carried out, lack an optical counterpart and we cannot exclude that some of these events are at $z \gtrsim 5$. A second scenario is that XRF are normal GRB seen off-axis (*e.g.*, [15] for a review). Let us assume that the only difference between the two classes is the viewing angle. This is equivalent to the unification scenario of Seyfert galaxies in the strong form. Again, under this assumption, the flux of the X-ray (and optical) afterglow observed at 12 hours should be substantially fainter than observed. In particular, both for the homogenous and for the universal jet models [4] find that the observed value of the afterglow ratio requires a maximum angle of a few degrees. In conclusion, the average property X-ray afterglows of XRF appears too bright to be consistent with a single origin, either in terms of off-axis jet or high-z scenario. One possibility is that we are missing a significant fraction of faint XRF and it is hoped that this population could be probed with more data by HETE2 and SWIFT. In order to assess alternative scenarios for the prompt emission [17], predictions on the afterglow properties need to be made.

* * *

I would like to thank B. Gendre, M. De Pasquale, A. Corsi, A. Galli and V. D'Alessio for inputs on this paper.

REFERENCES

[1]   Butler N. R., Marshall H. L., Ricker G. R. *et al.*,*ApJ*, **597** (2003) 1010.
[2]   Chevalier R. A. and Li Z., *ApJ*, **536** (2000) 195.
[3]   Chevalier R. A., Li Z. and Fransson C., *ApJ*, **606** (2004) 369.
[4]   D'Alessio V. and Piro L., these proceedings, 2005.
[5]   De Pasquale M., Piro L., Perna R. *et al.*, *ApJ*, **5092** (2003) 1018.
[6]   Djorgovski S. G., Frail D. A., Kulkarni S. R. *et al.*,*ApJ*, **562** (2001) 654.
[7]   Fox D. W., Price P. A., Soderberg A. M. *et al.*,*ApJ*, **586** (2003) L5.
[8]   Frontera F., Amati L., Costa E. *et al.*,*ApJS*, **127** (2000) 59.
[9]   Fynbo J. U., Jensen B. L., Gorosabel J. *et al.*, *A&A*, **369** (2001) 373.
[10] Galli A. and Piro L., these proceedings, 2005.
[11] B. Gendre *et al.*, these proceedings, 2005.
[12] Gendre B., Piro L. and De Pasquale M., *A&A*, **424** (2004) L27.
[13] Heise J., in 't Zand J., Kippen M. and Woods P., in *GRBs in the Afterglow Era*, edited by E. Costa, F. Frontera and J. Hjorth (ESO-Springer) 2001, pp. 16–21.
[14] Jakobsson P., Hjorth J., Fynbo J. P. U. *et al.*, *ApJ*, **617** (2004) L21.
[15] Lamb D., these proceedings, 2005.
[16] Lazzati D., Ramirez-Ruiz E. and Rees M. J., *ApJ*, **572** (2002) L57.
[17] Mochkovitch R., Daigne F., Barraud C. and Atteia J.-L., in *Third Rome workshop on GRBs in the Afterglow Era*, edited by M. Feroci, F. Frontera, N. Masetti and L. Piro, Vol. **312** (ASP) 2004, pp. 381-384.
[18] Panaitescu A. and Kumar P. s., *ApJ*, **571** (2002) 779.
[19] Perna R. and Loeb A., *ApJ*, **501** (1998) 467.
[20] Piro L., in *Third Rome workshop on GRBs in the Afterglow Era*, edited by M. Feroci, F. Frontera, N. Masetti and L. Piro, Vol. **312** (ASP) 2004, pp. 149-156.
[21] Piro L., De Pasquale M., Soffitta P. *et al.*,*ApJ*, **623** (2005) 314.
[22] Piro L., Costa E., Feroci M. *et al.*, *ApJ*, **514** (1999) L73.
[23] Piro L., Frail D., Gorosabel J. *et al.*, *ApJ*, **577** (2002) 680.
[24] Price P. A., Berger E., Reichart D. E. *et al.*, *ApJ*, **572** (2002) L51.
[25] Protassov R., van Dyk D. A., Connors A. *et al.*,*ApJ*, **571** (2002) 545.
[26] Reeves J. N., Watson D., Osborne J. L. *et al.*, *Nature*, **416** (2002) 512.
[27] Sako M., Harrison F. A. and Rutledge R. E., *ApJ*, **623** (2005) 973.
[28] Re'Em Sari and Tsvi Piran, *ApJ*, **520** (1999) 641.
[29] Soffitta P., De Pasquale M., Piro L. and Costa E., in *Third Rome workshop on GRBs in the Afterglow Era*, edited by M. Feroci, F. Frontera, N. Masetti and L. Piro, Vol. **312** (ASP) 2004, pp. 23-28.
[30] Watson D., Reeves J. N., Hjorth J. *et al.*, *ApJL*, **595** (2003) L29.
[31] Watson D., Reeves J. N., Osborne J. *et al.*,*A&A*, **393** (2002) L1.
[32] Wheaton W. A., Dunklee A. L., Jacobsen A. S. *et al.*,*ApJ*, **438** (1995) 322.